Scottish Universities Environmental Research Centre

OSL investigations at Hardisty, Alberta, Canada

February 2015

T.C. Kinnaird[1], K. Munyikwa[2] and D.C.W. Sanderson[1]

[1]SUERC, East Kilbride, Scotland, UK
[2]Athabasca University, 1 University Drive, Athabasca, Alberta, T8N 1T3, Canada

East Kilbride Glasgow G75 0QF Telephone: 01355 223332 Fax: 01355 229898

University of Glasgow
The University of Glasgow, charity number SC004401

The University of Edinburgh is a charitable body, registered in Scotland, with registration number SC005336

Summary

This report is concerned with optically stimulated luminescence (OSL) dating investigations of sediments associated with, and enclosing artefacts of First Nations historic significance in the Battle River Valley area, near Hardisty, east central Alberta. The OSL ages reported here provide chronological control to the archaeological investigations at this site, led by Rob Wondrasek, which have identified thousands of historical artefacts, including projectile points and lithic fragments indicative of occupation. The investigations were commissioned by Enbridge, ahead of the construction of the Edmonton-Hardisty Pipeline, and form one part of a historic resources impact assessment study, to characterise the archaeological site, and evaluate/mitigate the impact of the pipeline related excavations. This report describes the background to the investigation, sampling, and luminescence analysis undertaken to generate sediment chronologies for the Hardisty sediment stratigraphies.

Ken Munyikwa visited the archaeological investigations at Hardisty in June 2014 to sample key stratigraphic units within the sediment stratigraphies for OSL dating. Samples were collected from two profiles: from strata encompassing the artefact-bearing horizon, and from strata immediately beneath and overlying this horizon, thus providing terminus post quem (TPQ) and terminus ante quem (TAQ) on the age of this unit. Samples were submitted to the luminescence laboratories at SUERC for dating in August 2014. All samples were subjected to laboratory preparation of sand-sized quartz, and purity checked by scanning electron microscopy. Dose rates for the bulk sediment were evaluated using analyses of the uranium, thorium and potassium concentrations obtained by high resolution gamma spectrometry coupled with beta dose rate measurement using thick source beta counting. Equivalent doses were determined by OSL from 64 aliquots of quartz per sample using the quartz single-aliquot-regenerative (SAR) procedure. The material exhibited good OSL sensitivity and produced acceptable SAR internal quality control performance. Dose distributions from the aliquots were examined using radial plotting methods. All samples revealed some heterogeneity in their equivalent dose distribution, reflecting variable bleaching at deposition and indicating that each sample enclosed mixed-age materials. Age estimates were based on the weighted mean estimate of the stored dose, which weights the stored dose estimate towards the lowest population of equivalent doses, potentially representing the better bleached (at deposition) component.

The quartz OSL ages reported herein for the sand sequences at Hardisty-1 and Hardisty-2, have provided the first means to assess the temporal distribution of artefacts within the Hardisty profiles, and furthermore provide TPQ and TAQ for the inferred occupational phases. The sediment chronologies established for each profile are internally coherent, spanning at HD-01 from 7.8 ± 0.7 ka (SUTL2692) to 11.7 ± 0.5 ka (SUTL2694), and at HD-02 from 4.5 ± 0.2 ka (SUTL2695) to 8.7 ± 0.5 ka (SUTL2697; Table 4-1). TPQ for the occupation of the Hardisty site is provided by SUTL2697 at 8.7 ± 0.5 ka. TAQ for the occupation of the Hardisty site is provided by SUTL2695 at 4.5 ± 0.2 ka.

Contents

Summary i
1. Introduction 1
2. Sampling 1
3. Quartz SAR measurements 4
3.1. Sample preparation 4
3.1.1. Water contents 4
3.1.2. HRGS and TSBC Sample Preparation 4
3.1.3. Quartz mineral preparation 4
3.2. Measurements and determinations 4
3.2.1. Dose rate determinations 4
3.2.2. Quartz SAR luminescence measurements 5
3.3. Results 6
3.3.1. Dose rates 6
3.3.2. Single aliquot equivalent dose determinations 7
3.3.3. Age determinations 8
4. Discussion and conclusions 10
5. References 11
Appendix A: Dose Response Curves i
Appendix B: Radial plots iv

List of figures

Figure 1-1: The location of the archaeology sites shown relative to Hardisty (*GoogleEarth image)* 1
Figure 2-1: Photographs of sampled sections: (a) HD01 and (b) HD02 2
Figure 2-2: IRSL (red) and OSL (blue) net signal intensities vs depth for sections HD-01 and HD-02 3

List of tables

Table 2-1: Sample descriptions, contexts and archaeological significance of SUTL2692-2697 2
Table 2-2: Luminescence screening results made with a portable OSL reader 3
Table 3-1: Activity and equivalent concentrations of K, U and Th determined by HRGS 6
Table 3-2: Infinite matrix dose rates determined by HRGS and TSBC. 6
Table 3-3: Water contents, and effective beta and gamma dose rates following water correction. 7
Table 3-4: SAR quality parameters. Standard errors given. 8
Table 3-5: OSL age determinations for samples SUTL2692-97 9
Table 4-1: Quartz SAR OSL age constraints 10

1. Introduction

This report is concerned with optically stimulated luminescence (OSL) dating investigations of sediment from archaeological sites located approximately 2 km southwest of Hardisty in east central Alberta (Canada). Enbridge commissioned this work ahead of the development of the Edmonton to Hardisty Pipeline Project, which entails the construction of a 36-inch diameter crude oil pipeline linking terminals in Edmonton and Hardisty. Excavation work for the project discovered archaeological artefacts in the pipeline's right-of-way at a site near Hardisty (Fig. 1-1). The work by the archaeologists forms part of a historic resources impact assessment study that is being carried out to characterize the archaeological site, evaluate the impact of the pipeline related excavations and to advise on any mitigative measures that may be considered necessary to minimise any deleterious effects arising from the pipeline activities.

Figure 1-1: The location of the archaeology sites shown relative to Hardisty (*GoogleEarth image)*

The trace of the Edmonton to Hardisty Pipeline is observed running c. WNW-ESE in the SW quadrant of the satellite image

The objective of the OSL investigation is to provide chronological control for the geo-archaeological and stratigraphic investigation of the sediment stratigraphies examined at Hardisty sites HD01 and HD02. Specifically, it aims to constrain terminus post quem (TPQ) and terminus ante quem (TAQ) for the artefact-bearing horizons in the sediment stratigraphies through dating the enclosing sediments.

2. Sampling

Sampling was undertaken by Ken Munyikwa in June 2014. The studied sections, HD01 and HD02, located approximately 5 m apart, encompass at depth sands enclosing multiple projectile points and lithic fragments indicative of human occupation. Samples were taken from the units above and beneath the artefact-bearing horizon, and also from the unit enclosing the finds. In section HD-01 (Fig. 2-1a), sands were sampled at depths of 175, 197 and 213 cm, enclosing the artefact-bearing horizon between 187 and 207 cm. The uppermost sample was taken just above the current water table (at c. 190 cm), whereas the lower samples were taken from

beneath the water table. In section HD-02 (Fig. 2-1b), the sand units were sampled at depths of 164, 179 and 194 cm, with the artefact bearing horizon between 169 and 189 cm. As in HD-01, the uppermost sample was taken just above the water table (at c. 175 cm), and the lower two samples beneath the water table.

The samples were submitted for dating at the SUERC luminescence laboratories in August 2014. A brief description of the samples is given in Table 2-1, together with the laboratory (SUTL) numbers assigned to each sample on arrival at the SUERC luminescence laboratories. Photographs of the sections (Fig. 2-1), together with luminescence profiling data obtained using portable OSL instrumentation (Table 2-2), were provided.

Table 2-1: Sample descriptions, contexts and archaeological significance of SUTL2692-2697

Field no.	SUTL no.	Context No.	Depth in profile /cm	Lithological description	Archaeological significance
HD01-OSL1	2692	1	175	sand unit (possibly aeolian)	overlies strata enclosing multiple projectile points (potentially early to mid-Holocene); provides TAQ for artefact-bearing horizon
HD01-OSL2	2693	2	197		unit contains multiple projectile points and lithic fragments indicative of human occupation
HD01-OSL3	2694	3	213		underlies strata enclosing multiple projectile points (potentially early to mid-Holocene); provides TPQ for artefact-bearing horizon
HD02-OSL1	2695	1	164		overlies strata enclosing multiple projectile points (potentially early to mid-Holocene); provides TAQ for artefact-bearing horizon
HD02-OSL2	2696	2	179		unit contains multiple projectile points and lithic fragments indicative of human occupation
HD02-OSL3	2697	3	194		underlies strata enclosing multiple projectile points (potentially early to mid-Holocene); provides TPQ for artefact-bearing horizon

Figure 2-1: Photographs of sampled sections: (a) HD01 and (b) HD02

Initial luminescence screening was undertaken by Ken Munyikwa to characterise the luminescence properties of the sediments surrounding the units sampled for dating (Table 2-2; Fig 2-2), including two additional samples 30 and 50 cm below the modern ground surface to provide modern material controls. In both profiles, IRSL signal intensities initially increase down section, but decrease in the lower part of the sequence. However, with the blue OSL signal, the signal intensities increase down section. A possible explanation for this trend is that, in both cases, the lower part of the section contains buried soils in which the feldspar component is significantly weathered to clays. Since luminescence measurements were conducted on bulk samples using a portable OSL reader, it would imply that the drop in the IRSL signal is a response of a fall in the feldspar content of the samples. The blue OSL signal which includes a quartz contribution does not display a similar drop because quartz is much more resistant to weathering.

Table 2-2: Luminescence screening results made with a portable OSL reader

Sample No.	Depth from surface / cm	IRSL (counts)[1]	OSL (counts)[1]
Hardisty Site 1			
HD01A-01	30	39053	83097
HD01A-02	50	104025	248249
HD01-01	137	121719	331473
HD01-02	157	128267	250960
HD01-03	177	108552	264526
HD01-04	197	100494	284436
HD01-05	213	108164	303184
Hardisty Site 2			
HD02-01	137	89735	212139
HD02-02	157	114250	253753
HD02-03	177	2220066	253539
HD02-04	197	82228	252217

[1]average of three aliquots

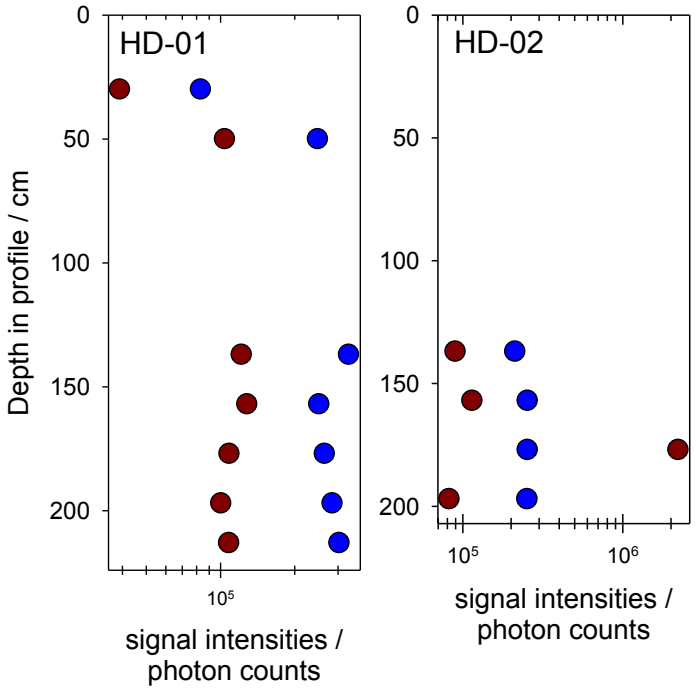

Figure 2-2: IRSL (red) and OSL (blue) net signal intensities vs depth for sections HD-01 and HD-02

3. Quartz SAR measurements

3.1. Sample preparation

All sample handling and preparation was conducted under safelight conditions in the SUERC luminescence dating laboratories.

3.1.1. Water contents

Bulk samples were weighed, saturated with water and re-weighed. Following oven drying at 50 °C to constant weight, the actual and saturated water contents were determined as fractions of dry weight. These data were used, together with information on field conditions to determine water contents and an associated water content uncertainty for use in dose rate determination.

3.1.2. HRGS and TSBC Sample Preparation

Bulk quantities of material, weighing c. 50g, were removed from each full dating sample for environmental dose rate determinations. This material was placed in an oven to dry to constant weight. Approximately 50g quantities of dried material from each sample were weighed into HDPE pots for a high-resolution gamma spectrometry (HRGS) measurement. Each pot was sealed with epoxy resin and left for 3 weeks prior to measurement to allow equilibration of ^{222}Rn daughters. A further 20 g of the dried material was used in thick source beta counting (TSBC; Sanderson, 1988).

3.1.3. Quartz mineral preparation

Approximately 20g of material was removed for each tube and processed for luminescence measurements to obtain sand-sized quartz grains. Each sample was wet sieved to obtain the 90-150 and 150-250 μm fractions. The 150-250 μm sub-sample was treated with 1 M hydrochloric acid (HCl) for 10 minutes, 15% hydrofluoric acid (HF) for 15 minutes, and 1 M HCl for a further 10 minutes. The HF-etched sub-samples were then centrifuged in sodium polytungstate solutions of ~2.51, 2.58, 2.62, and 2.74 gcm^{-3}, to obtain concentrates of potassium-rich feldspars (2.51-2.58 gcm^{-3}), sodium feldspars (2.58-2.62 gcm^{-3}) and quartz plus plagioclase (2.62-2.74 gcm^{-3}). The selected quartz fraction was then subjected to further HF and HCl washes (40% HF for 10mins, followed by 1M HCl for 10 mins). All materials were dried at 50°C and transferred to Eppendorf tubes. The 40%HF-etched, 2.62-2.74 gcm^{-3} 'quartz' fractions were dispensed to 10mm stainless steel discs for measurement. 64 aliquots were produced for all samples.

3.2. Measurements and determinations

3.2.1. Dose rate determinations

Dose rates were measured in the laboratory using HRGS and TSBC. Full sets of laboratory dose rate determinations were made for all samples.

HRGS measurements were performed using a 50% relative efficiency "n" type hyper-pure Ge detector (EG&G Ortec Gamma-X) operated in a low background lead shield with a copper liner. Gamma ray spectra were recorded over the 30 keV to 3 MeV range from each sample, interleaved with background measurements and measurements from SUERC Shap Granite standard in the same geometries. Sample counts were for 80ks. The spectra were analysed to determine count rates from the major line emissions from ^{40}K (1461 keV), and from selected nuclides in the U decay series (^{234}Th, ^{226}Ra + ^{235}U, ^{214}Pb, ^{214}Bi and ^{210}Pb) and the Th decay series (^{228}Ac, ^{212}Pb, ^{208}Tl) and their statistical counting uncertainties. Net rates and activity concentrations for each of these nuclides were determined relative to Shap Granite by weighted combination of the individual lines for each nuclide. The internal consistency of nuclide specific estimates for U and Th decay series nuclides was assessed relative to measurement precision, and weighted combinations used to estimate mean activity concentrations (Bq kg^{-1}) and elemental concentrations (% K and ppm U, Th) for the parent activity. These data were used to determine infinite matrix dose rates for alpha, beta and gamma radiation.

Beta dose rates were also measured directly using the SUERC TSBC system (Sanderson, 1988). Count rates were determined with six replicate 600 s counts on each sample, bracketed by background measurements and sensitivity determinations using the Shap Granite secondary reference material. Infinite-matrix dose rates were calculated by scaling the net count rates of samples and reference material to the working beta dose rate of the Shap Granite (6.25 ± 0.03 mGy a^{-1}). The estimated errors combine counting statistics, observed variance and the uncertainty on the reference value.

The dose rate measurements were used in combination with the assumed burial water contents, to determine the overall effective dose rates for age estimation. Cosmic dose rates were evaluated by combining latitude and altitude specific dose rates (0.19 ± 0.01 mGy a^{-1}) for the site with corrections for estimated depth of overburden using the method of Prescott and Hutton (1994).

3.2.2. **Quartz SAR luminescence measurements**

All measurements were conducted using a Risø DA-15 automatic reader equipped with a ^{90}Sr/^{90}Y β-source for irradiation, blue LEDs emitting around 470 nm and infrared (laser) diodes emitting around 830 nm for optical stimulation, and a U340 detection filter pack to detect in the region 270-380 nm, while cutting out stimulating light (Bøtter-Jensen et al., 2000). For each sample, equivalent dose determinations were made on sets of 64 aliquots per sample, using a single aliquot regeneration (SAR) sequence (cf Murray and Wintle, 2000). According to this procedure, the OSL signal level from an individual disc is calibrated to provide an absorbed dose estimate (the equivalent dose) using an interpolated dose-response curve, constructed by regenerating OSL signals by beta irradiation in the laboratory. To assess the dependence of equivalent dose on preheat, and the thermal stability of the OSL signal, eight different preheat temperatures were investigated (200, 210, 220, 230, 240, 250, 260 and 270°C). Sensitivity changes which may occur as a result of readout, irradiation and preheating (to remove unstable radiation-induced signals) are monitored using small test doses after each regenerative dose. Each measurement is standardised to the test dose response determined immediately after its readout, to

compensate for observed changes in sensitivity during the laboratory measurement sequence. For the purposes of interpolation, the regenerative doses are chosen to encompass the likely value of the equivalent (natural) dose. A repeat dose point is included to check the ability of the SAR procedure to correct for laboratory-induced sensitivity changes (the 'recycling test'), a zero dose point is included late in the sequence to check for thermally induced charge transfer during the irradiation and preheating cycle (the 'zero cycle'), and an IR response check is included to assess the magnitude of non-quartz signals. Regenerative dose response curves were constructed using doses of 2.5, 5, 10 and 50 Gy, with a test dose of 2 Gy.

3.3. Results

3.3.1. Dose rates

HRGS results are shown in Table 3-1, both as activity concentrations (i.e. disintegrations per second per kilogram) and as equivalent parent element concentrations (in % and ppm), based in the case of U and Th on combining nuclide specific data assuming decay series equilibrium.

Table 3-1: Activity and equivalent concentrations of K, U and Th determined by HRGS

SUTL no.	Activity Concentration[a] / Bq kg^{-1}			Equivalent Concentration[b]		
	K	U	Th	K / %	U / ppm	Th / ppm
2692	369 ± 16	7 ± 1.0	9 ± 1.0	1.19 ± 0.05	0.54 ± 0.07	2.32 ± 0.25
2693	382 ± 16	8 ± 1.0	14 ± 1.1	1.24 ± 0.05	0.66 ± 0.08	3.37 ± 0.26
2694	355 ± 15	10 ± 1.1	10 ± 1.0	1.15 ± 0.05	0.80 ± 0.09	2.53 ± 0.25
2695	361 ± 15	7 ± 0.9	11 ± 1.0	1.17 ± 0.05	0.60 ± 0.08	2.62 ± 0.25
2696	354 ± 16	8 ± 1.0	10 ± 1.0	1.14 ± 0.05	0.65 ± 0.08	2.46 ± 0.24
2697	395 ± 11	9 ± 0.5	13 ± 0.4	1.28 ± 0.03	0.70 ± 0.04	3.15 ± 0.10

[a]Shap granite reference, working values determined by David Sanderson in 1986, based on HRGS relative to CANMET and NBL standards.

[b]Activity and equivalent concentrations for U, Th and K determined by HRGS (Conversion factors based on NEA (2000) decay constants): 40K: 309.3 Bq kg^{-1} %K^{-1}, 238U: 12.35 Bq kg^{-1} ppmU^{-1}, 232Th: 4.057 Bq kg^{-1} ppm Th^{-1}.

Infinite matrix alpha, beta and gamma dose rates from HRGS are listed for all samples in Table 3-2, together with infinite matrix beta dose rates from TSBC.

Table 3-2: Infinite matrix dose rates determined by HRGS and TSBC.

SUTL no.	HRGS, dry[a] / mGy a^{-1}			TSBC, dry / mGy a^{-1}
	Alpha	Beta	Gamma	
2692	3.22 ± 0.28	1.14 ± 0.04 (3.9%)	0.47 ± 0.02 (4.2%)	1.22 ± 0.05
2693	4.33 ± 0.29	1.22 ± 0.05 (3.7%)	0.55 ± 0.02 (3.7%)	1.25 ± 0.05
2694	4.09 ± 0.30	1.14 ± 0.04 (3.8%)	0.50 ± 0.02 (4.0%)	1.01 ± 0.05
2695	3.61 ± 0.28	1.13 ± 0.04 (3.8%)	0.49 ± 0.02 (4.0%)	1.01 ± 0.04
2696	3.63 ± 0.28	1.11 ± 0.04 (4.0%)	0.48 ± 0.02 (4.1%)	1.27 ± 0.05
2697	4.26 ± 0.13	1.25 ± 0.03 (2.3%)	0.55 ± 0.01 (2.0%)	1.19 ± 0.05

[a]based on dose rate conversion factors in Aikten (1983) and Sanderson (1987)

The water content measurements with assumed values for the average water content during burial are given in Table 3-3. The table also lists the gamma dose rate from the HRGS after application of a water content correction. Effective dose rates to the HF

etched 200 μm quartz grains are given for the gamma dose rate and beta dose rate (the mean of the TSBC and HRGS data, accounting for water content and grain size).

Table 3-3: Water contents, and effective beta and gamma dose rates following water correction.

SUTL no.	Water content / %			Effective Dose Rate / mGy a^{-1}		
	Fractional	Saturated	Assumed	Beta[a]	Gamma	Total[b]
2692	20.4	21.1	20.6 ± 2	0.89 ± 0.05	0.38 ± 0.02	1.44 ± 0.06
2693	24.3	29.5	25.6 ± 3	0.88 ± 0.05	0.43 ± 0.02	1.48 ± 0.07
2694	26.4	28.5	27.0 ± 2	0.76 ± 0.05	0.38 ± 0.02	1.32 ± 0.06
2695	21.2	23.8	21.9 ± 2	0.79 ± 0.05	0.39 ± 0.02	1.36 ± 0.06
2696	21.3	21.5	21.3 ± 2	0.89 ± 0.05	0.39 ± 0.02	1.45 ± 0.06
2697	24.2	24.5	24.3 ± 2	0.89 ± 0.04	0.43 ± 0.01	1.49 ± 0.06

[a] Effective beta dose rate combining water content corrections with inverse grain size attenuation factors obtained by weighting the 200 μm attenuation factors of Mejdahl (1979) for K, U, and Th by the relative beta dose contributions for each source determined by Gamma Spectrometry.
[a] includes a cosmic dose contribution

3.3.2. **Single aliquot equivalent dose determinations**

For equivalent dose determination, data from single aliquot regenerative dose measurements were analysed using the Risø TL/OSL Viewer programme to export integrated summary files that were analysed in MS Excel and SigmaPlot. Composite dose response curves were constructed from selected discs and for each of the eight preheating groups from each sample, and used to estimate equivalent dose values for each individual disc and their combined sets. Dose response curves for each of the eight preheating temperature groups and the combined data were determined using a fit to exponential function (SUTL2692-96) or a fit to exponential + linear function (SUTL2697; Appendix A). The equivalent dose was then determined for each aliquot using the corresponding exponential fit parameters.

Single aliquots were rejected from further analysis based on the test dose sensitivity check, SAR criteria checks, the robust mean, feldspar contamination and radial plots. Table 3-4 summarises the quality evaluation checks on the SAR data (once filtered); the mean sensitivity of each aliquot and sensitivity change, the recycling ratio and zero dose response.

The distribution in equivalent dose values was examined using radial plotting methods (Appendix B). All samples revealed some heterogeneity in their equivalent dose distributions. It is noted that the sands in each sequence enclose mixed-age components, and indeed the dose distributions obtained for all 6 dating samples show some aliquots which tail towards higher apparent ages (Table 3-5). It has been argued that the best estimate of the true burial dose with such sediments is the lowest measured dose, or population of doses. Age estimates were based on the weighted mean estimate of stored dose for SUTL2692 - SUTL2696, and on the robust mean estimate for SUTL2697.

Table 3-4: SAR quality parameters. Standard errors given.

SUTL No.	Sensitivity (counts/Gy)	Sensitivity change (%)	Recycling Ratio	Zero Dose (Gy)	IRSL response (%)
2692	289 ± 60	12 ± 4	1.00 ± 0.02	0.3 ± 0.3	13.9 ± 12.3
2693	621 ± 99	3 ± 1	1.01 ± 0.02	0.1 ± 0.1	1.4 ± 1.0
2694	1033 ± 142	-8 ± -2	0.99 ± 0.02	0.2 ± 0.2	3.3 ± 1.0
2695	2466 ± 1306	1 ± 0	1.01 ± 0.02	0.2 ± 0.1	15.8 ± 2.9
2696	541 ± 91	11 ± 3	1.00 ± 0.02	0.1 ± 0.0	1.0 ± 0.3
2697	668 ± 100	8 ± 1	1.01 ± 0.02	0.4 ± 0.1	13.7 ± 0.7

3.3.3. **Age determinations**

The total dose rate is determined from the sum of the equivalent beta and gamma dose rates, and the cosmic dose rate. Age estimates are determined by dividing the equivalent stored dose by the dose rate. Uncertainty on the age estimates is given by combination of the uncertainty on the dose rates and stored doses, with an additional 5% external error. Table 3-5 lists the total dose rate, stored dose and corresponding age of the sample.

Table 3-5: OSL age determinations for samples SUTL2692-97

Field ID.	SUTL No.	Dose Rate (mGy a^{-1})	Comments on Equivalent Dose Distribution	Stored Dose (Gy)	Age / ka	Calendar years / yrs BC
HD01-OSL1	2692	1.44 ± 0.06	broad equivalent dose distribution: 28 aliquots cluster around the weighted mean 11.9 ± 1.3 (0.9) Gy; 14 aliquots (>12 % rel. err) tail to a lower stored dose value ~ 5 Gy; 22 aliquots tail to a higher stored dose value ~ 13 Gy	11.9 ± 0.9	7.8 ± 0.7	5830 ± 670
HD01-OSL2	2693	1.48 ± 0.07	broad equivalent dose distribution: 35 aliquots cluster around the weighted mean 12.2 ± 0.6 (0.2) Gy; 16 aliquots tail to a lower stored dose value ~ 7-8 Gy; some aliquots tail to a higher stored dose value ~ 13-14 Gy	12.2 ± 0.2	7.8 ± 0.4	5820 ± 350
HD01-OSL3	2694	1.32 ± 0.06	broad equivalent dose distribution: 23 aliquots cluster around the weighted mean 16.3 ± 0.1 Gy; 6 aliquots tail to a lower stored dose value ~ 9 Gy; 7 aliquots tail to a higher stored dose value ~ 24-25 Gy	16.3 ± 0.1	11.7 ± 0.5	9720 ± 520
HD02-OSL1	2695	1.36 ± 0.06	broad equivalent dose distribution: 20 aliquots cluster around the weighted mean 6.5 ± 0.1 Gy; 8 aliquots (>15% rel. err) tail to a lower stored dose value ~ 4 Gy; 15 aliquots tail to a higher stored dose value ~ 11-13 Gy	6.5 ± 0.1	4.5 ± 0.2	2530 ± 210
HD02-OSL2	2696	1.45 ± 0.06	broad equivalent dose distribution: 42 aliquots cluster around the weighted mean 10.3 ± 0.1 Gy; 8 aliquots (>15% rel. err) tail to a lower stored dose value ~ 4 Gy; some aliquots (>15% rel. err) tail to a higher stored dose value ~ 12-16 Gy	10.3 ± 0.1	6.8 ± 0.3	4780 ± 300
HD02-OSL3	2697	1.49 ± 0.06	broad equivalent dose distribution: 13 aliquots cluster around the weighted mean 10.1 ± 0.1 Gy, whereas 29 aliquots cluster around the robust mean 13.7 ± 0.6 Gy; 4 aliquots tail to a lower stored dose value ~ 5 Gy; some aliquots tail to a higher stored dose value ~ 20 Gy	13.7 ± 0.6	8.7 ± 0.5	6700 ± 480

4. Discussion and conclusions

The quartz OSL ages reported here for the sand sequences at Hardisty-1 and Hardisty-2, provide the means to assess the temporal distribution of artefacts within the two sections, and furthermore provide TPQ and TAQ for the inferred occupational phase. The sediment chronologies established for each profile are internally coherent, spanning at HD-01 from 7.8 ± 0.7 ka (SUTL2692) to 11.7 ± 0.5 ka (SUTL2694), and at HD-02 from 4.5 ± 0.2 ka (SUTL2695) to 8.7 ± 0.5 ka (SUTL2697; Table 4-1). TPQ for the occupation of the Hardisty site is provided by SUTL2697 at 8.7 ± 0.5 ka. TAQ for the occupation of the Hardisty site is provided by SUTL2695 at 4.5 ± 0.2 ka.

Table 4-1: Quartz SAR OSL age constraints

SUTL no.	Field no.	Age / ka	Calendar years / yrs BC
Hardisty section HD-01			
2692	HD01-OSL1	7.8 ± 0.7	5830 ± 670
2693	HD01-OSL2	7.8 ± 0.4	5820 ± 350
2694	HD01-OSL3	11.7 ± 0.5	9720 ± 520
Hardisty section HD-02			
2695	HD02-OSL1	4.5 ± 0.2	2530 ± 210
2696	HD02-OSL2	6.8 ± 0.3	4780 ± 300
2697	HD02-OSL3	8.7 ± 0.5	6700 ± 480

There is scope for further age modelling including the use of Bayesian methods to refine the TPQ age limits.

5. References

Aitken, M.J., 1983, Dose rate data in SI units: PACT, v. 9, p. 69–76.

Bøtter-Jensen, L., Bulur, E., Duller, G.A.T., and Murray, A.S., 2000, Advances in luminescence instrument systems: Radiation Measurements, v. 32, p. 523-528.

Mejdahl, V., 1979, Thermoluminescence daing: Beta-dose attenuation in quartz grains Archaeometry, v. 21, p. 61-72.

Murray, A.S., and Wintle, A.G., 2000, Luminescence dating of quartz using an improved single-aliquot regenerative-dose protocol: Radiation Measurements, v. 32, p. 57-73.

NEA, 2000, The JEF-2.2 Nuclear Data Library: Nuclear Energy Agency, Organisation for economic Co-operation and Development. JEFF Report, v. 17.

Prescott, J.R., and Hutton, J.T., 1994, Cosmic ray contributions to dose rates for luminescence and ESR dating: Large depths and long-term time variations: Radiation Measurements, v. 23, p. 497-500.

Sanderson, D.C.W., 1987, Thermoluminescence dating of vitrified Scottish Forts: Paisley, Paisley college.

—, 1988, Thick source beta counting (TSBC): A rapid method for measuring beta dose-rates: International Journal of Radiation Applications and Instrumentation. Part D. Nuclear Tracks and Radiation Measurements, v. 14, p. 203-207.

Appendix A: Dose Response Curves

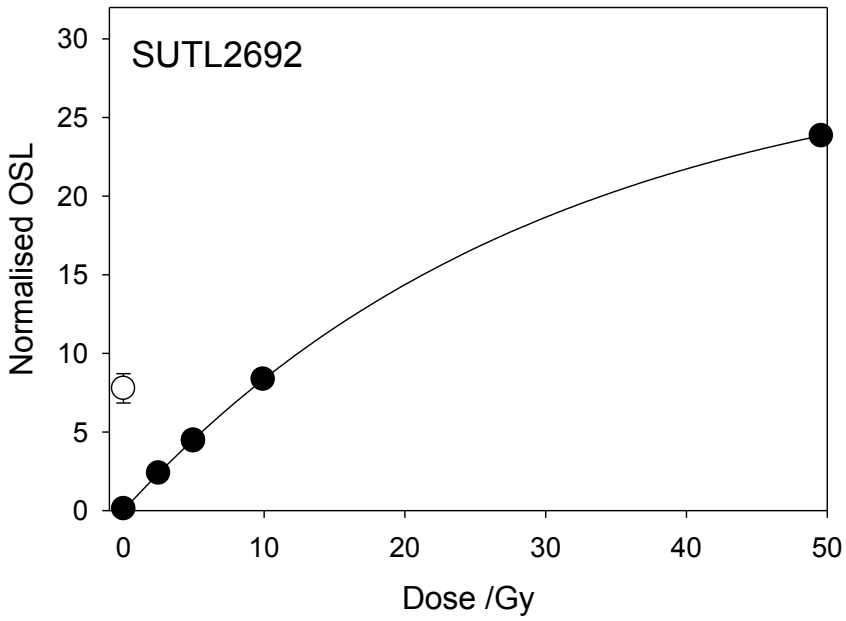

Figure A-1: Composite dose response curve for SUTL2692
Lx = 2.5, 5, 10 and 50 Gy;
Tx = 1 Gy

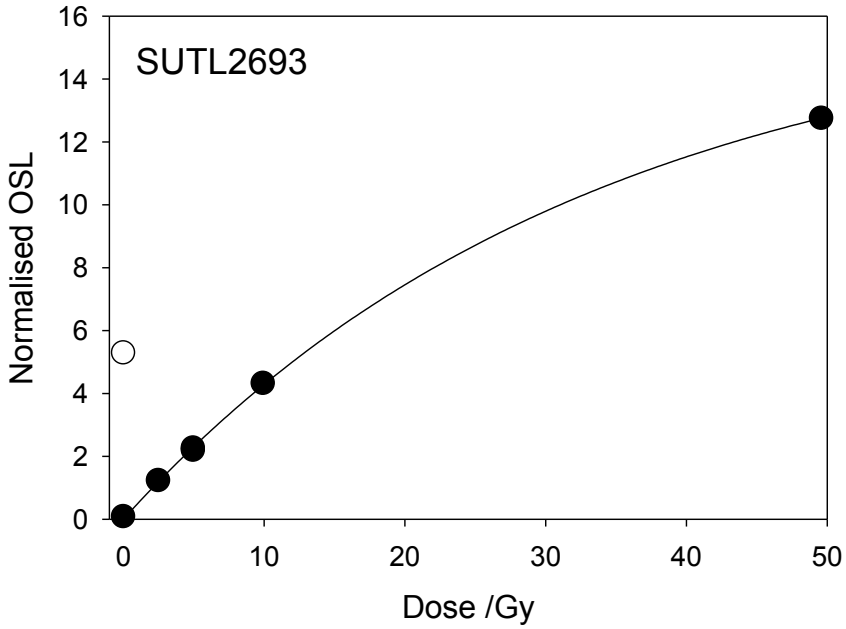

Figure A-2: Composite dose response curve for SUTL2693
Lx = 2.5, 5, 10 and 50 Gy;
Tx = 2Gy

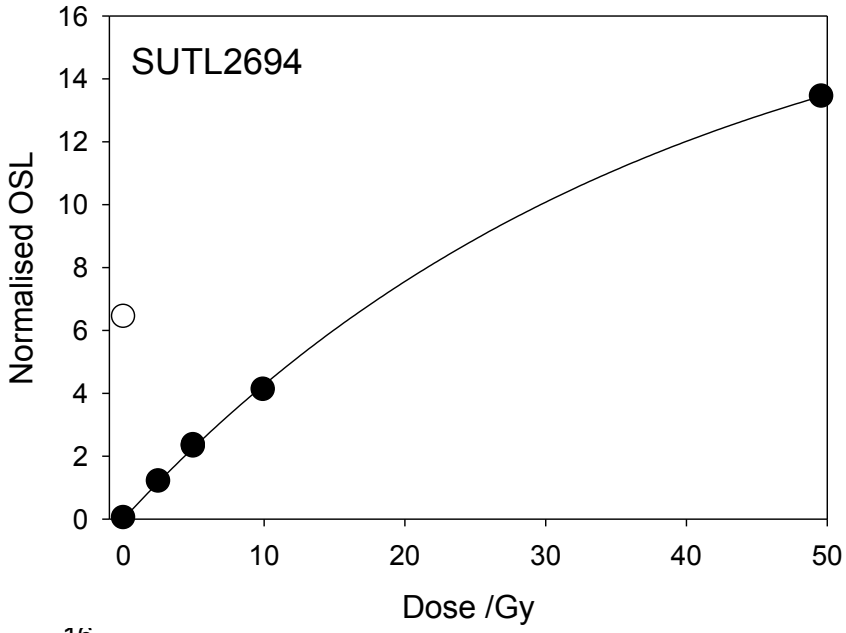

Figure A-3: Composite dose response curve for SUTL2694
Lx = 2.5, 5, 10 and 50 Gy;
Tx = 2Gy

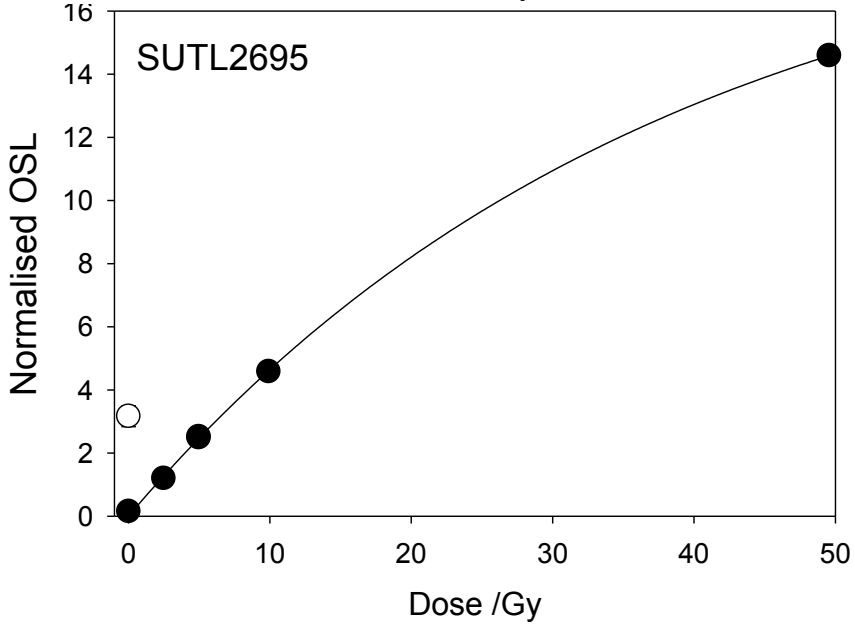

Figure A-4: Composite dose response curve for SUTL2695
Lx = 2.5, 5, 10 and 50 Gy;
Tx = 2Gy

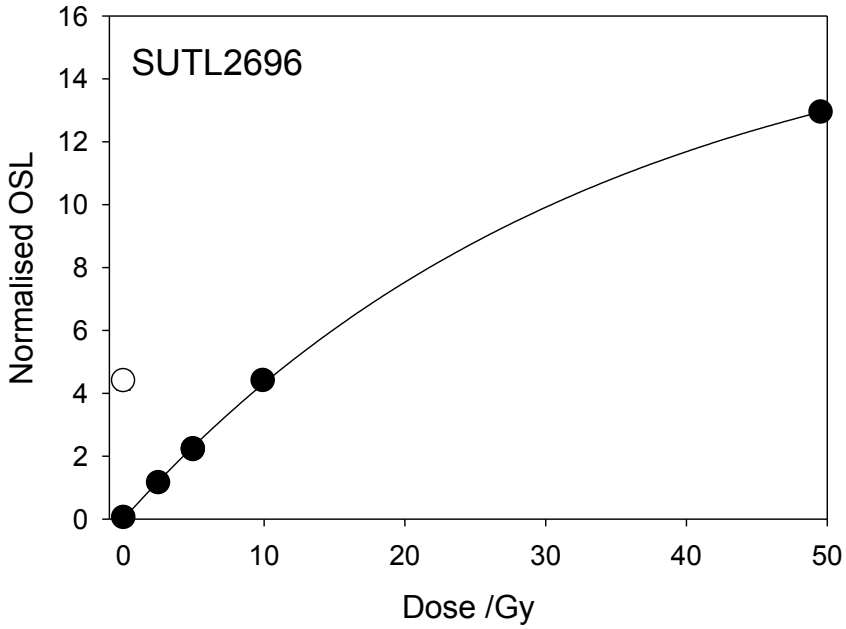

Figure A-5: Composite dose response curve for SUTL2696
Lx = 2.5, 5, 10 and 50 Gy;
Tx = 2Gy

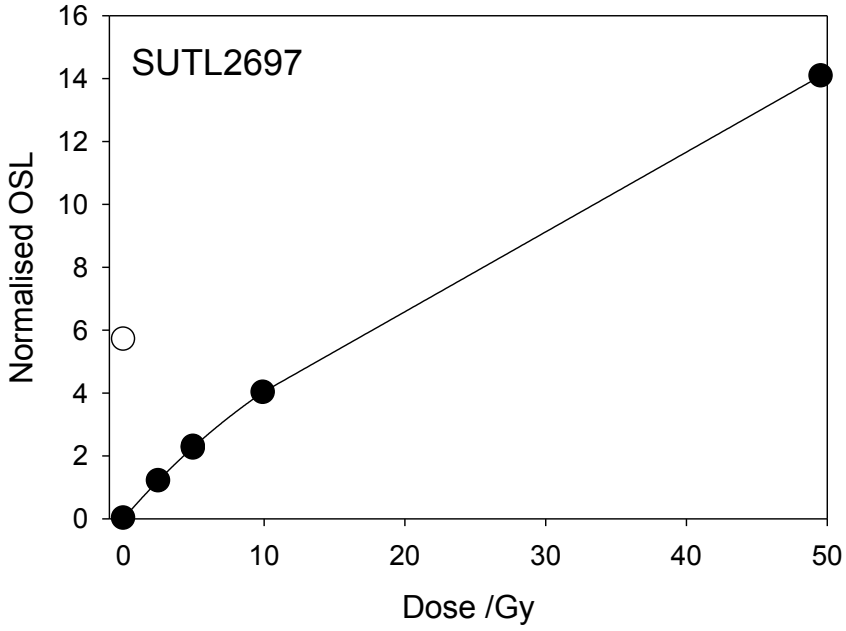

Figure A-6: Composite dose response curve for SUTL2697
Lx = 2.5, 5, 10 and 50 Gy;
Tx = 2Gy

Appendix B: Radial plots

Figure B-1: Radial plot for SUTL2692

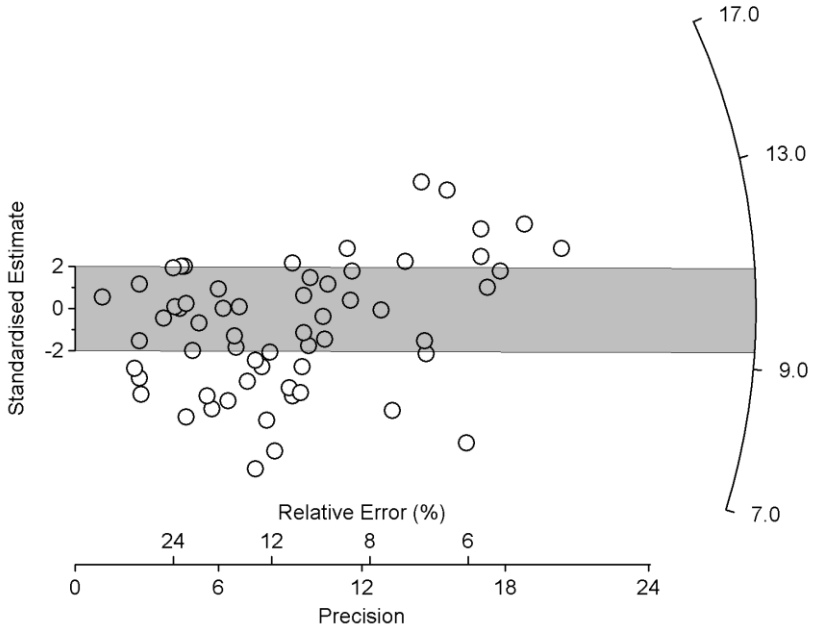

Figure B-2: Radial plot for SUTL2693

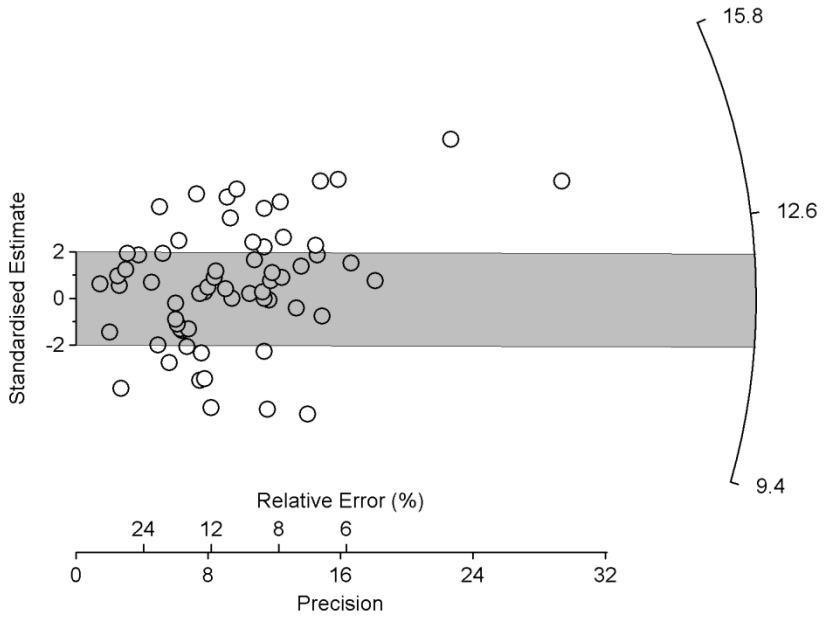

Figure B-3: Radial plot for SUTL2694

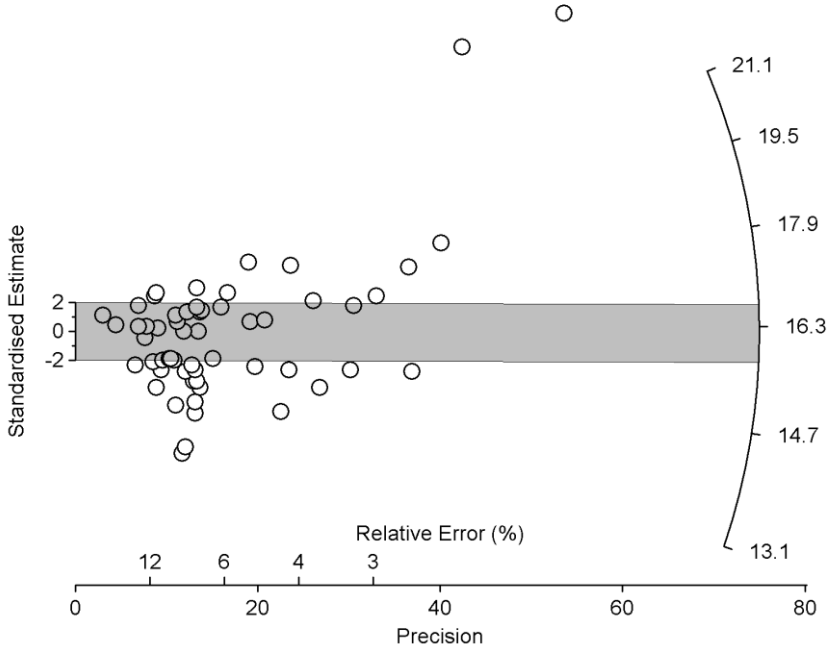

Figure B-4: Radial plot for SUTL2695

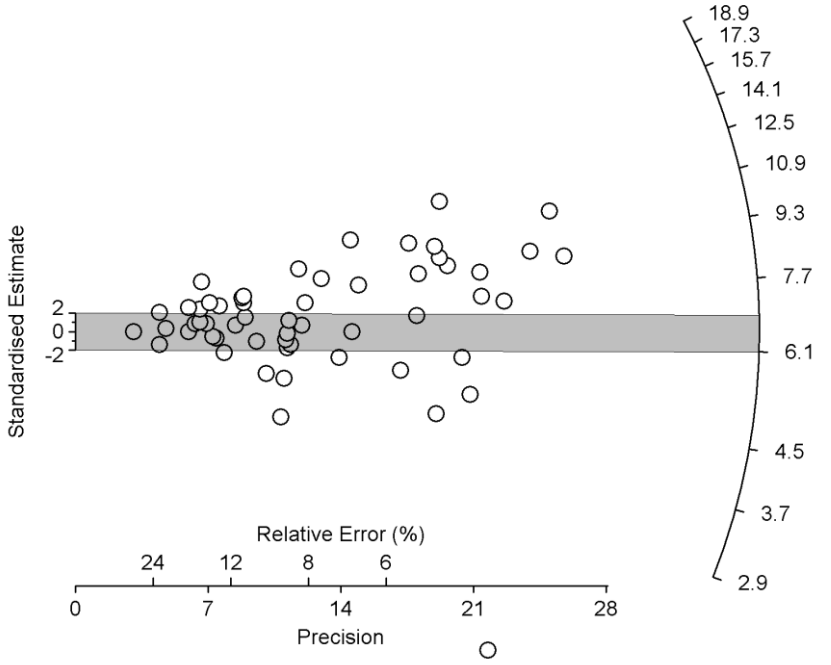

Figure B-5: Radial plot for SUTL2696

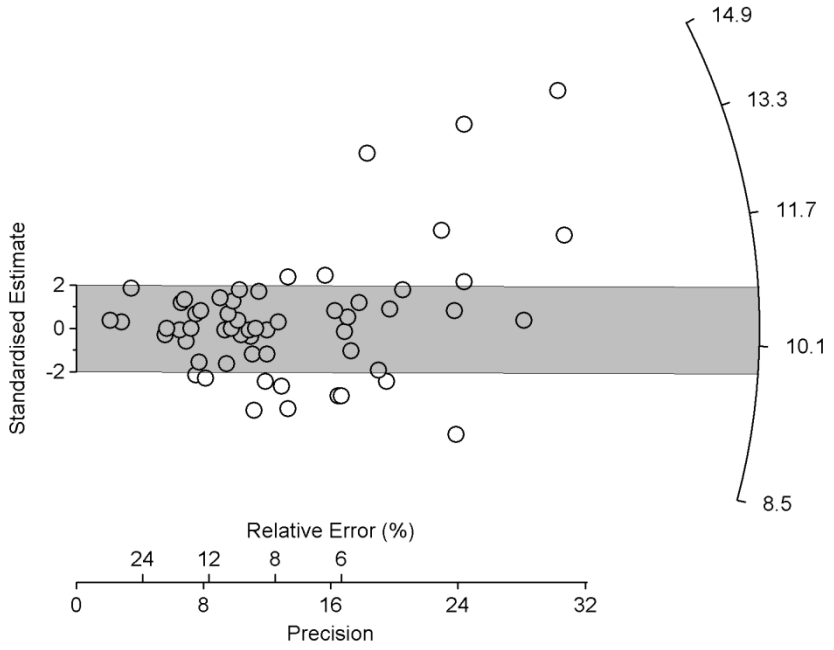

Figure B-6: Radial plot for SUTL2697